

# On the cloud observations in JAXA's next coming satellite missions

Takashi Y. Nakajima<sup>a</sup>, Takashi M. Nagao<sup>a</sup>, Husi Letu<sup>a</sup>, Haruma Ishida<sup>b</sup>, Kentaroh Suzuki<sup>c</sup>

<sup>a</sup>Research and Information Center (TRIC), Tokai University  
2-28-4, Tomigaya, Shibuya-ku, Tokyo, 151-0063, Japan.

<sup>b</sup>Graduate School of Science and Engineering, Yamaguchi University  
2-16-1, Tokiwadai, Ube City, Yamaguchi Pref., 755-8611, Japan

<sup>c</sup>Jet Propulsion Laboratory, California Institute of Technology  
M/S 233-300, 4800 Oak Grove Drive, Pasadena, CA 91109, USA

## ABSTRACT

The use of JAXA's next generation satellites, the EarthCARE and the GCOM-C, for observing overall cloud systems on the Earth is discussed. The satellites will be launched in the middle of 2010-era and contribute for observing aerosols and clouds in terms of climate change, environment, weather forecasting, and cloud revolution process study. This paper describes the role of such satellites and how to use the observing data showing concepts and some sample viewgraphs. Synergistic use of sensors is a key of the study. Visible to infrared bands are used for cloudy and clear discriminating from passively obtained satellite images. Cloud properties such as the cloud optical thickness, the effective particle radii, and the cloud top temperature will be retrieved from visible to infrared wavelengths of imagers. Additionally, we are going to combine cloud properties obtained from passive imagers and radar reflectivities obtained from an active radar in order to improve our understanding of cloud evolution process. This is one of the new techniques of satellite data analysis in terms of cloud sciences in the next decade. Since the climate change and cloud process study have mutual beneficial relationship, a multispectral wide-swath imagers like the GCOM-C SGLI and a comprehensive observation package of cloud and aerosol like the EarthCARE are both necessary.

**Keywords: GCOM-C, EarthCARE, Cloud, Aerosol, Satellite Remote Sensing, Climate Change**

# 1. INTRODUCTION

Since clouds exert an important influence on the planet's water and energy balances and processes (IPCC 2007)<sup>1</sup>, more observations of clouds with understanding of their lifecycle are required. There are many numbers of studies of observing cloud optical and microphysical properties from aircraft (e.g. Nakajima et al. 1991<sup>2</sup>, Asano et al. 1995<sup>3</sup>, Painemal and Zuidema 2011<sup>4</sup>) and satellite (e.g. Han et al. 1994<sup>5</sup>, Nakajima and Nakajima 1995<sup>6</sup>, Kawamoto et al. 2001<sup>7</sup>). Han et al. (1994) retrieved Cloud Optical Thickness (COT) and Cloud Droplet effective Radius (CDR) for near-globally from the nadir looking NOAA AVHRR radiance data using 0.6-, 3.7-, and 11- $\mu\text{m}$  bands. One of the interesting features obtained from Han's results is that they revealed the contrast of effective radii between continental area and coastal-ocean area. The global averaged effective radius is smaller in continental area (CDR=8.5 $\mu\text{m}$ ) and large in coastal zone (CDR=11.8 $\mu\text{m}$ ). Nakajima and Nakajima (1995) developed an algorithm that retrieved cloud properties using whole AVHRR scene and analyzed the aerosol-cloud interaction. Kawamoto et al (2001) improved the Nakajima's algorithm so that the water vapor effects implicitly included in the measured radiances are explicitly corrected using the effective water vapor parameters obtained from objective analysis data. An important mission of the cloud remote sensing is to obtain long-term records of cloud type, state, and cloud properties that contribute to the climate change study.

One of the recent trends of the satellite-borne cloud observations are interpretation of satellite-derived cloud properties, e.g. COT and the discrepancy in the retrieved CDR with different wavelengths in use (hereafter, the CDR discrepancy). This trend is motivated by the cloud lifecycle process study. For instance, Platnick (2000)<sup>8</sup> investigated the CDR discrepancy using different wavelengths such as 3.7 $\mu\text{m}$ , 2.1 $\mu\text{m}$  and 1.6 $\mu\text{m}$  in terms of penetration efficiency of each ray in clouds from the cloud top. Nakajima et al. (2010a)<sup>9</sup> demonstrated and confirmed that both vertical inhomogeneity of clouds and droplet size distribution can generate the CDR discrepancy. Zhang and Platnick (2011)<sup>10</sup> suggested a new interpretation that the sub-pixel horizontal inhomogeneity causes the CDR discrepancy. These demonstrations and results suggest that the satellite-retrieved CDR have not only information of the cloud droplet size but also degree of cloud inhomogeneity and hopefully some hints of cloud growing process. The CloudSat and the CALIPSO present a new epoch in cloud observation community with the purpose of revealing the particle transition, from cloud condensation nuclei (CCN), cloud and drizzle particles, and rain drops, thus, it is expected to present vital hints for solving the cloud inhomogeneities. For instance, the CFODD (see section 3.2), a new visualization method of the radar reflectivities shows transition of cloud growth, from cloud droplet mode to rain mode via drizzle mode, very clearly. Indeed combined use of the passive and active sensor is quite important for the process study of the cloud revolution.

Here, Japan Aerospace Exploration Agency (JAXA) is developing new satellites that contribute cloud sciences, the Earth Clouds, Aerosols and Radiation Explorer (EarthCARE) and the Global Change Observation Mission (GCOM) series. The EarthCARE satellite is a comprehensive package for observing aerosols, clouds, and radiation, using cloud radar, lidar, multispectral imager, and broadband radiometer. Doppler capability of the cloud radar investigates vertical motion of cloud particles. The GCOM-C Second generation Global Imager (SGLI) is a multispectral imager that has 19

spectral bands from near UV to thermal infrared. Advantages of the SGLI are, wide-swath that contributes global-scale observation, two polarization bands for detecting aerosols over land area, and long-term monitoring continued from past satellite missions. It is expected that the coupled use of these sensors reveal details of aerosol and cloud evolution process.

In this paper, we'd like to introduce the JAXA's next coming satellites that contribute to the aerosols and clouds observation, analysis method and algorithm, and mention about mutual benefit between these satellites.

## 2. SATELLITE MISSIONS AND SENSORS

### 2.1 GCOM-C SGLI

The SGLI is the next-generation imager to follow the Midori-II Global Imager (GLI). It will be aboard on the GCOM-C satellite that is scheduled to launch around 2015. The SGLI consists of the Visible and Near-infrared Radiometer (VNR) and Infrared Scanner (IRS) (see Table 1). SGLI-VNR is divided into polarized and unpolarized sections. Among them, 0.67, 0.87, 1.63, 1.38, and 10.8, 12.0- $\mu\text{m}$  bands will be used for cloudy and clear discrimination (cloud detection, cloud screening) of the SGLI images. 0.67, 1.05, 1.63, 2.2, and 10.8- $\mu\text{m}$  bands are used for retrieving cloud properties. Recently, we are developing algorithms called CLAUDIA (CLOUD and Aerosol Unbiased Decision Intellectual Algorithm)<sup>11-13</sup> and CAPCOM (Comprehensive Analysis Program for Cloud Optical Measurements)<sup>6-7</sup> for cloud detection (CLAUDIA) and retrieving cloud properties (CAPCOM).

Table 1 GCOM-C SGLI band specifications

Band #	Wavelength ( $\mu\text{m}$ )	IFOV (km)	Band #	Wavelength ( $\mu\text{m}$ )	IFOV (km)
VN1	0.380	0.25	P1	0.670	1.0
VN2	0.412	0.25	P2	0.865	1.0
VN3	0.443	0.25	SW1	1.05	1.0
VN4	0.490	0.25	SW2	1.38	1.0
VN5	0.530	0.25	SW3	1.63	0.25
VN6	0.565	0.25	SW4	2.21	1.0
VN7	0.670	0.25	T1	10.8	0.5
VN8	0.670	0.25	T2	12.0	0.5
VN9	0.763	1.0			
VN10	0.865	0.25			
VN11	0.865	0.25			

## 2.2 EarthCARE CPR and MSI

The EarthCARE Multispectral Imager (MSI) is also a visible-to-infrared imager that has seven bands from visible to infrared. It is equipped on the satellite together with two active sensors, namely, Cloud Profiling Radar (CPR) and ATmospheric backscatter LIDar (ATLID), and a passive radiometer, the Broad Band Radiometer (BBR). The EarthCARE has been developed through collaborations among the JAXA, the National Institute of Information and Communications Technology (NICT) in Japan, and the European Space Agency (ESA).

Different from a wide-swath visible-to-infrared imager SGLI, the MSI is relatively a compact sensor aiming coincident and collocated observation of clouds together with active sensors, CPR and ATLID. Thus, the cross track swath of the MSI is 150-km whereas 1,400-km swath of the GCOM-C. The MSI detects clouds and retrieves cloud properties. All of the MSI bands will be used for cloudy and clear discrimination. 0.67-, 1.67-, 2.21-, and 10.8 $\mu$ m are used for retrieving cloud properties. The CPR is an active radar that enable to observe the vertical structure of clouds along nadir footprint of the spacecraft using 94 GHz frequency with Doppler capability of 1 m/s accuracy. The EarthCARE CPR is the first cloud profiling radar with Doppler.

Table 2 EarthCARE MSI (Imager) specifications

Band #	Wavelength ( $\mu$ m)	IFOV (km)
1	0.67	0.5
2	0.87	0.5
3	1.67	0.5
4	2.21	0.5
5	8.8	0.5
6	10.8	0.5
7	12.0	0.5

Table 3 EarthCARE CPR (Radar) specifications

CPR Specification	
Altitude	450 km
Frequency	94 GHz
Resolution	500 m
Height range	-0.5~20 km
Sensitivity	-35 dBZ
Doppler accuracy	1 m/s

## 3. SYNERGISTIC USE OF THE PASSIVE AND ACTIVE SENSORS

### 3.1 Cloud properties obtained from passive imagers

As we briefly described in the previous section, cloud optical and microphysical properties are retrieved from the passive imagers. Indeed, we are going to retrieve cloud optical thickness (COT), cloud droplet effective radii (CDR), cloud top temperature (CTT) from the MSI images.

The principle of the retrieval can be explained by the difference in the imaginary index of refraction by liquid water in non-absorbing bands such 0.67 and 1.05 ( $10^{-9} \sim 10^{-6}$ ) and absorbing bands 1.6 and 2.1 ( $10^{-5} \sim 10^{-3}$ ). The optical rays in non-absorbing wavelength can go through deeply layer of the clouds so that channel1 has information about cloud optical property of whole cloud layers, whereas the ray of absorbing absorbed by cloud particles due to moderately large imaginary index of refraction so that these bands has information of cloud droplet size at the near cloud top.

Figure 1 shows radiative transfer simulation results obtained with a fixed geolocation angles (satellite zenith angle 45 degs, solar zenith angle 50 degs, and relative azimuthal angle 120 degs). The figure illustrates relationship between cloud properties (cloud optical thickness COT and cloud droplet effective particle radii CDR) and expected measured radiance from satellite sensors. The CAPCOM is, actually, an algorithm that retrieves COT and CDR etc using a concept shown in Fig. 1. In order to apply the CAPCOM for globally observations, the CAPCOM has some pre-calculated look up tables (databases) of the expected measured radiance with wide variation of the cloud properties and geolocation angles.

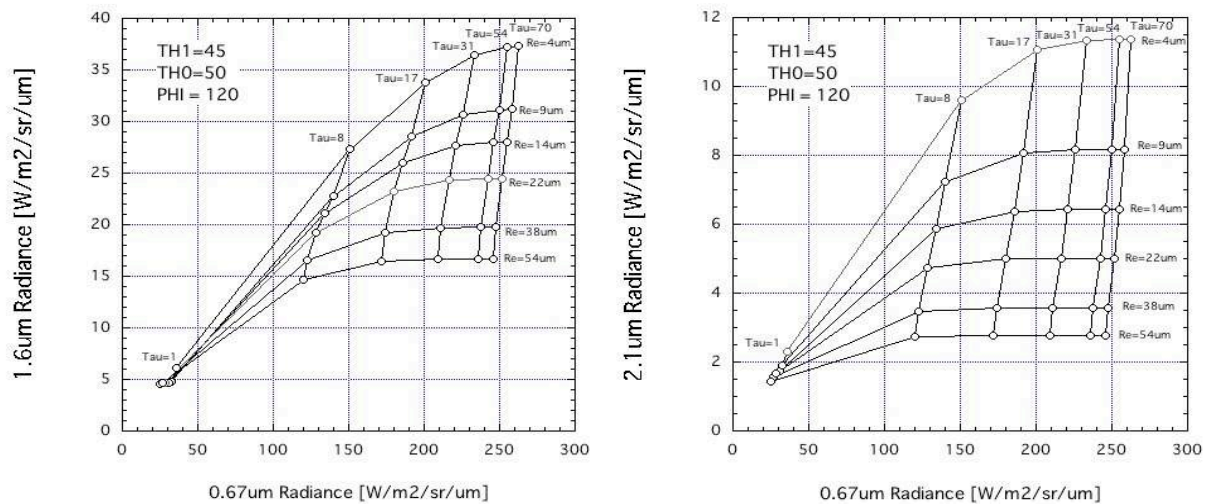


Fig. 1 Simulation of reflected solar radiances in 0.67- $\mu\text{m}$  band and 1.6- $\mu\text{m}$  band (left), 0.67- $\mu\text{m}$  band and 2.1- $\mu\text{m}$  band as a function of cloud optical thickness (COT) and cloud droplet effective radii (CDR).

### 3.2 The CFODD

The CFODD is a new visualization method for the CPR radar reflectivities invented by Nakajima et al. (2010b)<sup>14</sup> and Suzuki et al. (2010)<sup>15</sup>. Here, we would like to explain what's CFODD, how do we generate the CFODD, in this article, because we have been asked to many scientists about CFODD since 2010. There are several different points in CFODD from a conventional visualization method called the CFAD (Contoured Frequency by Altitude Diagram). First the CFODD need a total cloud optical thickness (COT) that is coincidentally retrieved by the passive imager, whereas

the CFAD can be generated by cloud radar data alone. In this regards, the CFODD is exposed by a synergistic use of the active radar and the passive imager and considered to include significant information about cloud state and evolution process. Second, the vertical axis of the CFODD is the In-Cloud-Optical-Depth (ICOD) whereas the geometrical altitude from ground base in CFAD. ICOD is a kind of a vertical structure of clouds in terms of cloud optical property, so ICOD=0 indicates cloud top. We used 2B-TAU product of the CloudSat project (Polinsky 2008)<sup>16</sup> in the first version of the CFODD to obtain ICOD. However, optical depth at each layer bin was depended on the CPR reflectivities  $Z$ , thus, the vertical and horizontal axes were not independent. In the version 2, Suzuki et al. (2010)<sup>15</sup> introduced a method for the cloud optical depth slicing obtained from an adiabatic condensation growth assumption, namely,

$$ICOD(h) = COT \left[ 1 - (h/H)^{5/3} \right], \quad (1)$$

where,  $h$  and  $H$  are geometrical height of cloud layer and cloud total geometrical thickness assumed by radar reflectivity profile, respectively. Figure 2 is a schematic illustration to explain how do we construct the CFODD using passive and active remote sensing (the sample is an synergistic use of the Aqua MODIS imager and CloudSat CPR radar on the A-Trans constellation system). The left part of Fig.2 is a result of CDR and COT obtained from the MODIS and CloudSat CPR radar reflectivities along the nadir footprint of satellites. The CFODD shows frequency of occurrence of the CPR reflectivities. Once ICOD is calculated by Eq.(1) for every cloud observation then a occurrence is counted up at a bin of target ICOD and a radar reflectivities.

One of interesting feature appears in the CFODD grouped by CDR that obtained from a passive imager. Fig.2 illustrates a CFODD that generated by gathering radar reflectivities of clouds that have MODIS-derived CDR between 14 $\mu$ m and 16 $\mu$ m only. Indeed, this CFODD show a typical vertical structure of clouds that have MODIS-derived CDR between 14 $\mu$ m and 16 $\mu$ m. Similarly, the CFODDs of other grouping can be generated by different range of CDR as shown in Fig. 3, e.g. CDR between 6-8 $\mu$ m, 8-10 $\mu$ m, 10-12 $\mu$ m, 12-14 $\mu$ m, 14-16 $\mu$ m (= the case of Fig.2), 16-18 $\mu$ m, 18-20 $\mu$ m, 20-25 $\mu$ m and 25-30 $\mu$ m. Nine panels of the CFODD are shown in Figure 3. Amazingly, the figure showed that the CFODDs obviously follow the transition of the cloud droplet growth as MODIS-derived CDR values increasing, from cloud particle mode (-20 dBZ), drizzle mode (-10 dBZ), and rain (10 dBZ), monotonically. Despite the MODIS-derived CDR is only a representing of the particle size at the upper layer of clouds, the CFODD clearly present vertical structure of clouds.

The CFODD suggests that the passively obtained cloud properties have information of cloud evolution process. It is needed to investigate more in details focusing different meteorological condition such in ocean and land areas. Different convection, for example, will generate different CFODD so that the Doppler capability of the EarthCARE will contribute to further CFODD study.

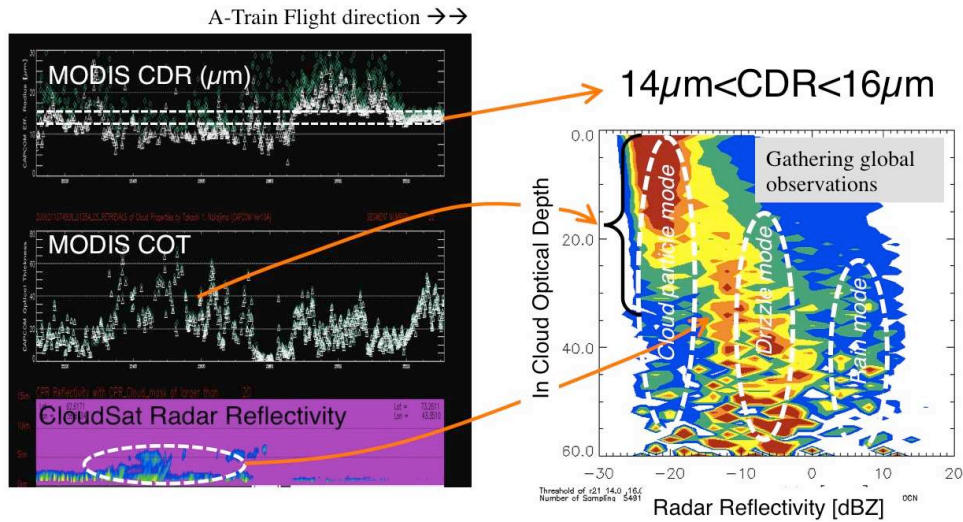


Fig. 2 Schematic illustration to explain how do we construct the CFODD using passive and active remote sensing (the sample is an synergistic use of the Aqua MODIS imager and CloudSat CPR radar on the A-Trains constellation system).

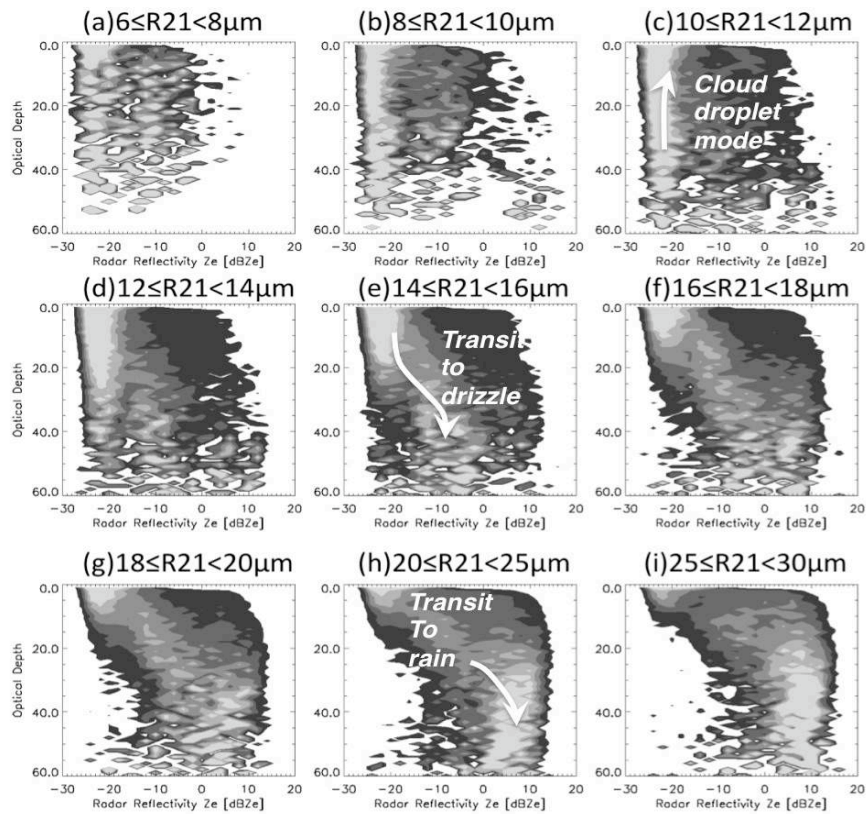


Fig. 3 Contoured Frequency by Optical Depth Diagram (CFODD) classified by CDR(in this figure, R21) with threshold CDR values of 6, 8, 10, 12, 16, 18, 20, 25, and 30  $\mu\text{m}$  for the ocean area. (Cited from Nakajima et al. 2010b<sup>14</sup> with depicted by a gray scale and rearrangement)

#### 4. CONCLUDING REMARKS

JAXA has been planned and developed some satellite series that contribute cloud-aerosol sciences in terms of climate change, environmental study, weather forecasting and so on. This paper describes the role of such satellite observations and how to use these satellite data, by focusing two of JAXA's next coming missions, the EarthCARE and the GCOM-C. Recently, the satellite missions are aiming not only obtaining a long term records (longer than decades) of cloud distribution state (type and amount etc.) and cloud properties for the climate change study but also aiming cloud evolution process study. Figure 4 illustrates concept of the JAXA's next coming satellite for contributing climate change study and cloud process study. As shown this figure, two kinds of studies have mutual beneficial relationship. For instance, a long history of passive sensing of clouds motivates active sensing of clouds. Actually, cloud amount obtained from passive sensing can be validated using active sensing efficiently. The CDR discrepancy, noted in the section 1 is examined by using active sensing as well. Vice versa, a wide-swath of the passive sensing fills data gap that appeared in the active sensing. Therefore a multispectral wide-swath imager like the GCOM-C SGLI and a comprehensive observation package of cloud and aerosol like EarthCARE are both necessary.

We didn't mention about other important missions in JAXA, in this paper, such as GCOM-W Advanced Microwave Scanning Radiometer 2 (AMSR2) series and the Global Precipitation Measurement (GPM) that measures cloud water and precipitation. It is obvious that they are also important satellites because cloud water and precipitation are tightly connected with the process of CCN to rain as mentioned in this paper.

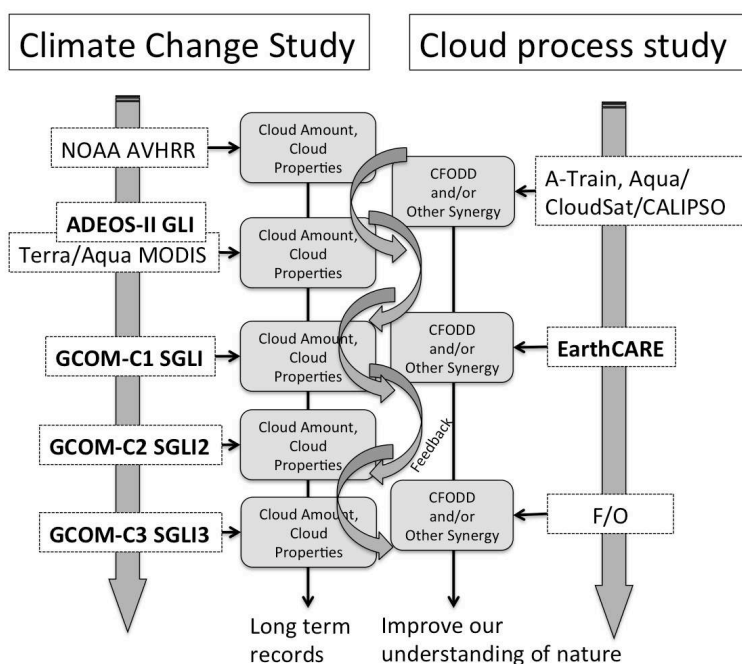


Fig. 4 Concept of the JAXA's satellite (**bold**) for contributing Climate Change Study and Cloud Process Study

## Acknowledgements

This research was supported by JAXA GCOM-C and EarthCARE project, partly funded NASA Contracts NNX07AR11G and NAS5-99237, and supported by Grant-in-Aid #18684025 and #22340133 provided by the Ministry of Education, Science, Sports and Culture, Japan. Part of the research was carried out at the Jet Propulsion Laboratory, California Institute of Technology, under a contract with the National Aeronautics and Space Administration.

## REFERENCES

- [1] Solomon, S. "IPCC (Intergovernmental Panel on Climate Change) (2007), *Climate Change 2007: The Physical Science Basis.*" Cambridge Univ. Press, Cambridge, UK and New York, USA., 996 pp (2007).
- [2] Nakajima, T. M.D.King, J. D. Spinhirne, and L. F. Radke, "Determination of the optical thickness and effective radius of clouds from reflected solar radiation measurements. Part II: Marine stratocumulus observations.," *J. Atmos. Sci.*, 48, 728-750 (1991).
- [3] Asano, S. M. Shiobara, and A. Uchiyama, "Estimation of cloud physical parameters from airborne solar spectral reflectance measurements for stratocumulus clouds.," *J. Atmos. Sci.*, 52, 3556-3576 (1995).
- [4] Painemal, D., and P. Zuidema, "Assessment of MODIS cloud effective radius and optical thickness retrievals over the Southeast Pacific with VOCALS-REx in situ measurements," *J. Geophys. Res.*, 116, D24206, doi:10.1029/2011JD016155 (2011).
- [5] Han, Q., W. B. Rossow, and A. A. Lacis, "Near-global survey of effective droplet radii in liquid water clouds using ISCCP data.," *J. Climate*, 7, 465-497 (1994).
- [6] Nakajima, T. Y. and T. Nakajima, "Wide-area determination of cloud microphysical properties from NOAA AVHRR measurement for FIRE and ASTEX regions," *J. Atmos. Sci.*, 52, 4043-4059 (1995).
- [7] Kawamoto, K., T. Nakajima, and T. Y. Nakajima, "A global determination of cloud microphysics with AVHRR remote sensing.," *J. Climate*, 14, 2054-2068 (2001).
- [8] Platnick, S., "Vertical photon transport in cloud remote sensing problems," *J. Geophys. Res.*, 105(D18), 22,919–22,935, doi:10.1029/2000JD900333 (2000).
- [9] Nakajima, T. Y., K. Suzuki, G. L. Stephens, "Droplet Growth in Warm Water Clouds Observed by the A-Train. Part I: Sensitivity Analysis of the MODIS-Derived Cloud Droplet Sizes.," *J. Atmos. Sci.*, 67, 1884–1896, doi: 10.1175/2009JAS3280.1 (2010a).
- [10] Zhang, Z., and S. Platnick, "An assessment of differences between cloud effective particle radius retrievals for marine water clouds from three MODIS spectral bands.," *J. Geophys. Res.*, 116, D20215, doi:10.1029/2011JD016216 (2011)
- [11] Ishida, H., and T. Y. Nakajima, "Development of an unbiased cloud detection algorithm for a spaceborne multispectral imager.," *Journal of Geophysical Research-Atmospheres*, 114, doi:10.1029/2008JD010710 (2009).
- [12] Ishida, H., T. Y. Nakajima, T. Yokota, N. Kikuchi, and H. Watanabe, "Investigation of GOSAT TANSO-CAI cloud screening ability through an inter-satellite comparison.," *Journal of Applied Meteorology and Climate*, 50, 1571-1586 (2011)
- [13] Nakajima, T. Y., T. Tsuchiya, H. Ishida, and H. Shimoda, "Cloud detection performance of spaceborne visible-to-infrared multispectral imagers.," *Applied Optics*, 50, 2601-2616 (2011).
- [14] Nakajima, T. Y., K. Suzuki, and G. L. Stephens, "Droplet growth in warm water clouds observed by the A-Train. Part II: A Multi-sensor view.," *J. Atmos. Sci.*, 67, 1897-1907 (2010b).
- [15] Suzuki, K., T. Y. Nakajima, and G. L. Stephens "Particle growth and drop collection efficiency of warm clouds as inferred from joint CloudSat and MODIS observations.," *Journal of the Atmospheric Sciences*, 67, 3019-3032 (2010).
- [16] Polinsky, I. N., "Level2 cloud optical depth product process description and interface control document, CloudSat Project, A NASA Earth system science pathfinder mission.," CIRA Colorado State University, Fort Collins. (2008).